David M. Huang

Computational study of P3HT/C_{60}-fullerene miscibility

Australian Journal of Chemistry, 2014; 67(4):585-591

Originally Published at: http://dx.doi.org/10.1071/CH13518

Computational Study of P3HT/C_{60}-Fullerene Miscibility

David M. Huang[A,B]

[A] School of Chemistry and Physics, The University of Adelaide, SA 5005, Australia

[B] Email: david.huang@adelaide.edu.au

Classical molecular dynamics simulations and statistical thermodynamics are used to investigate the miscibility of blends of the conjugated polymer poly(3-hexylthiophene) (P3HT) and fullerene C_{60} for blend ratios typically used in organic photovoltaic devices over a range of temperatures. Depending on which of two slightly different simulation force fields is used, the calculations suggest that amorphous P3HT/fullerene blends are either miscible or immisicble under typical processing conditions. The former result is consistent with recent experiments and suggests that experimentally observed nano-scale phase separation is driven by polymer or fullerene crystallisation. But the inconsistency between the different force fields indicates that these blends are close to phase coexistence between the separated and homogeneously mixed phases and suggests that care must be taken in interpreting simulation data on P3HT/fullerene blends. These findings have implications for organic photovoltaics, in which the microstructure of conjugated-polymer/fullerene blends plays a crucial role in device performance.

Introduction

Solution-processed organic polymer-based solar cells have attracted growing interest because of their potential as low-cost and flexible alternatives to conventional silicon-based photovoltaics. Rapid strides have been made in the last two decades to improve their efficiency to the point that their use is becoming commercially viable.[1] The power conversion efficiency of polymer solar cells is sensitive to the microstructure of the photo-active layer.[1,2] This layer typically consists of a mixture of a conjugated polymer and a fullerene derivative, respectively, as electron donor and acceptor materials, which phase separates on the nano scale to form an interpenetrating bicontinuous network known as a bulk heterojunction.[2]

The small diffusion length of photo-induced electronic excited states (excitons) in organic materials limits the characteristic width of donor and acceptor domains to the ten-nanometre scale in efficient solar cells, while the photo-active layer typically needs to be hundreds of nanometres thick to absorb most of the incident light. The sensitivity of solar cell efficiency to the bulk heterojunction microstructure is in part due to the delicate balance between having donor and acceptor domains that are narrow enough for efficient dissociation of excitons into free charges at donor/acceptor interfaces and having percolating pathways in the donor and acceptor materials for free charges to travel through the photo-active layer to the electrodes.

Although polymer solar cell bulk heterojunctions are typically formed under non-equilibrium conditions, the equilibrium phase behaviour of the donor/acceptor mixture plays a key role in determining the final microstructure and provides an important control parameter for optimising device performance.[3–5] For example, the optimal polymer/fullerene blend ratio has been related to the eutectic composition of the blend[3] and solar cell performance has been correlated with fullerene miscibility in the polymer.[5] Evidence has also emerged recently that the conventional picture of the bulk heterojunction consisting only of domains of pure polymer and fullerene phases is overly simplistic, with the bulk heterojunction generally also containing an intermixed polymer/fullerene phase that has a significant impact on efficient charge generation and device performance[6,7]

These results suggest that partial miscibility of the polymer and fullerene, at least for amorphous components of the blend, may be the rule rather than the exception in polymer solar cells and may in fact be desirable for optimal device performance. Phase separation of the donor/acceptor blend in the bulk heterojunction, rather than being driven by immiscibility of the blend components, appears instead to be driven in many cases by crystallisation of either the fullerene[6] (in the case of polymers such as many low-band-gap push–pull polymers that do not readily crystallise[7]) or the polymer[8,9] (in the case of polymers such as poly(3-hexylthiophene) (P3HT) that form well-ordered crystalline phases).

P3HT is one of the most widely used conjugated polymers in organic photovoltaics and phenyl-C_{61}-butyric acid methyl ester (PCBM) the most widely used fullerene. Using transmission electron microscopy (TEM) and X-ray scattering, Kozub et al.[9] showed that blends of regiorandom P3HT (which does not crystallise) and PCBM are miscible for polymer volume fractions above 0.42. On the other hand, annealed films of 1:1 w/w blends of regioregular P3HT (which does crystallise) with PCBM were found to contain pure P3HT crystallites and PCBM-rich domains that contained approximately 45% P3HT by volume, indicating phase separation driven by a combination of P3HT crystallisation and the limited solubility of P3HT and PCBM.[9] From X-ray scattering and DSC, Kim and Frisbie[10] estimated the room-temperature solubility limit of PCBM in amorphous P3HT domains to be 50% by weight, with this value declining to 30% upon annealing to form semi-crystalline P3HT. Other measurements have shown significant, albeit lower, solubility of PCBM in P3HT. From fitting of scanning transmission X-ray microscopy (STXM) data of P3HT/PCBM films annealed at 140°C to a diffusion model, Watts et al.[11] estimated the PCBM concentration at the boundary of PCBM crystals to be 19% by volume, which was interpreted to be the solubility limit of PCBM in P3HT at this temperature. By fitting near-edge X-ray absorption fine structure (NEXAFS) spectra of P3HT:PCBM blends to a linear combination of spectra for the pure components, Collins et al.[12]

estimated the miscibility limit of PCBM in P3HT to increase from 16 to 21% for regiorandom P3HT and 4 to 11% for regioregular P3HT from 120 to 180°C. From differential scanning calorimetry (DSC) measurements of the the melting point depression of P3HT in P3HT/PCBM mixtures, Chen et al.[8] estimated the Flory–Huggins interaction parameter[13] between P3HT and PCBM to be -0.162, the negative value suggesting that amorphous P3HT/PCBM blends are highly miscible. On the other hand, using similar techniques Kozub et al.[9] measured Flory–Huggins parameter of 0.86 ± 0.09, indicating miscibility of amorphous P3HT/PCBM blends for certain blend compositions. (Incidentally, the analysis of P3HT/PCBM blend miscibility using Flory–Huggins theory[13] by Kozub et al.[9] is incorrect, as it does not account for the difference in monomer volume for P3HT and PCBM; accounting for this difference leads to a significantly lower miscibility than predicted by Kozub et al.[9].)

Thus, there is some uncertainty surrounding the inherent miscibility of conjugated-polymer/fullerene blends used in polymer solar cells. Computer simulation models can play an important role in elucidating the microstructure and phase behaviour of conjugated-polymer/fullerene bulk heterojunctions. But conventional atomistically detailed simulation models cannot easily be applied to studying structure formation on the characteristic 10-nm length scale of the donor and acceptor domains in bulk heterojunctions. For this reason, simplified models of polymer/fullerene blends that allow larger systems to be simulated over longer time scales than can be achieved with atomistic models, such as coarse-grained (CG) molecular models[14,15], have been developed. In these models, each monomer is represented by a small number of "superatoms" and the interactions between the sites are iteratively tuned so that all relevant local structural correlations (e.g. bond, angle, dihedral, and non-bonded pair distributions) in small-scale coarse-grained simulations match those in atomistic simulations of analogous systems. This structure-based coarse-graining procedure is typically carried out at a particular thermodynamic state point at which the blend system is homogeneous, as intermolecular site–site structural correlations are assumed to be spherically symmetric.

In contrast to the available experimental data, the coarse-grained models developed so far of P3HT/fullerene mixtures, namely P3HT/PCBM[15] and P3HT/C_{60}[14,16] blends, exhibit very low polymer/fullerene miscibility for the blend compositions typically used in solar cells, even though no polymer crystallization is evident in the simulations that have been carried out. The stark difference between the experimental and simulation observations raises questions about the accuracy of these coarse-grained models in describing the phase behaviour of P3HT/fullerene mixtures.

In this work, atomistic molecular dynamics (MD) simulations of blends of P3HT oligomers with the fullerene C_{60} (Fig. 1) are used to investigate the miscibility of P3HT/C_{60} mixtures for the blend ratios and processing conditions used for P3HT/fullerene bulk-heterojunction solar cells and statistical thermodynamical arguments are used to extrapolate the predictions for oligomer systems to the polymer chain lengths used in solar cells. The findings indicate that these mixtures are close to phase coexistence between the separated and homogeneously mixed phases and highlight the need to re-examine the parametrisation of simulation models of conjugated-polymer/fullerene blends to ensure that the equilibrium phase behaviour of these blends is correctly reproduced.

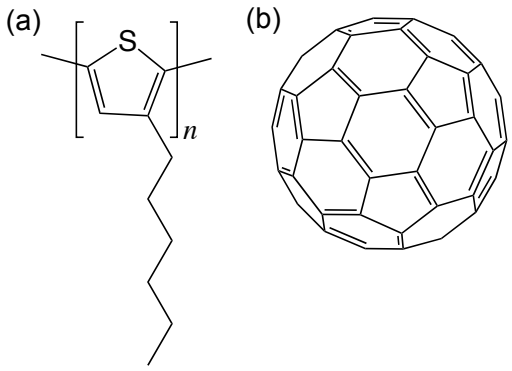

Figure 1: Chemical structures of (a) poly(3-hexylthiophene) (P3HT) and (b) C_{60}.

This work represents a first step towards using computer simulations to understand the factors that govern the the miscibility of fullerenes with P3HT and thus the simplest fullerene, C_{60}, has been used. Subsequent work is planned in which the P3HT/PCBM will be studied to compare more directly with available experimental thermodynamic data on P3HT/fullerene miscibility and to investigate the role of fullerene substituents on miscibility.

Computational Methods

Classical MD simulations of pure P3HT, pure C_{60}, and a P3HT/C_{60} mixture were carried out at various temperatures using the LAMMPS MD simulation package.[17] 108 C_{60} molecules were used in all simulations containing fullerene. The simulations containing P3HT used either 590 P3HT monomers or 59 regioregular P3HT decamers. For the mixture simulations, these values correspond to a 1:0.79 w/w P3HT:C_{60} blend ratio, which has the same mole ratio as the 1:1 w/w P3HT:PCBM blends typically used in P3HT-based organic solar cells. Constant temperature and pressure (NPT ensemble) simulations of all systems were carried out at 1 atm and 450, 500, 550, and 600 K. As points of reference, the melting temperature of pure P3HT is approximately 500 K[3,10] and thermal annealing to optimise the microstructure of P3HT/fullerene bulk heterojunctions is typically carried out between 400–450 K; temperatures below 450 K were not simulated as the P3HT decamer systems are essentially immobile on the simulation time scale for temperatures significantly below this value.

Unless otherwise stated, the simulations containing P3HT were started from an initial configuration of randomly positioned and oriented molecules, with the inter-monomer dihedral angle distribution taken from a Boltzmann distribution of the inter-monomer torsional potential. The simulations of the pure C_{60} systems were initiated from an fcc crystal lattice, the stable phase of C_{60} at all the temperatures simulated, which were well below the C_{60} melting point. Representative configurations from some of the simulations, which used cubic simulation boxes and periodic boundary conditions, are shown in Fig. 2. Total simulation times are given in Table 1.

The simulation model for P3HT is described in detail in Ref. 19. The simulation procedure and algorithms used are identical to those in Ref. 19.The P3HT model was adapted

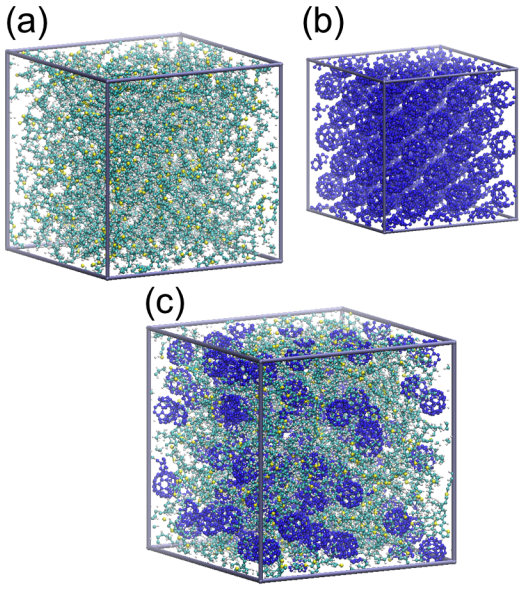

Figure 2: Simulation configurations from simulations at 500 K and 1 atm of (a) 59 P3HT decamers, (b) 108 C_{60} molecules, and (c) a mixture of 59 P3HT decamers and 108 C_{60} molecules using the Girifalco model [18] for C_{60}.

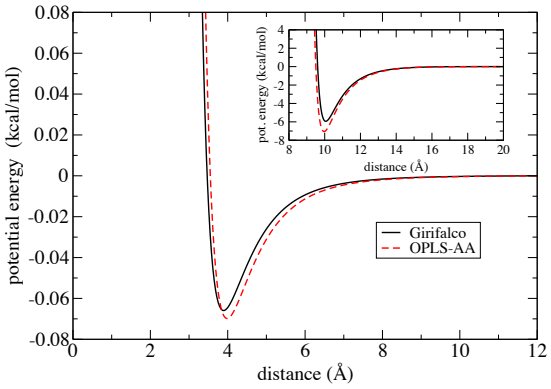

Figure 3: Carbon–carbon Lennard-Jones potential in Girifalco [18] (solid line) and OPLS-AA [21] (dashed line) force fields. *Inset*: Total C_{60}–C_{60} potential energy assuming a uniform density of carbon atoms over the surface of a sphere the size of the C_{60} molecule.

from a model of tetrathiophene [20] based on the OPLS-AA force field [21–23] that was found to agree well with experiments for structural and thermodynamic properties. To construct the P3HT model, the tetrathiophene model was augmented to include an inter-monomer torsional potential from density functional theory (DFT) calculations of alkyl-substituted oligothiophenes [24] and a hexyl side-chain with parameters from the OPLS-AA force field. The OPLS-AA (optimized potentials for liquid simulations all-atom) force field itself is a general force field that has been shown to describe accurately the condensed-phase structural and thermodynamic properties of a variety of organic molecules.

The OPLS-AA force field does not contain parameters specific to fullerenes. The generic parameters for aromatic carbon atoms bonded to other aromatic carbon atoms in the OPLS-AA force field are not entirely satisfactory for modelling C60, with the average carbon-carbon bond length underestimated by several percent [25] and the crystal density consequently overestimated by several percent. [18] On the other hand, the widely used C_{60} model of Girifalco [18] (described in detail in Ref. 14) has been parametrised to match experimental data for the heat of sublimation and lattice constant of C_{60} and has been found to closely match the experimental compressibility of an fcc crystal of C_{60}. The C_{60} non-bonded parameters in the Girifalco model are close to those in the OPLS-AA force field for aromatic carbon atoms, [21] with the Lennard-Jones diameter and well depth in the two force field differing by only 2% and 6%, respectively. Nevertheless, combining the Girifalco model for C_{60} with the OPLS-AA-based model for P3HT is not optimal. To investigate the force-field dependence of the simulation results, both the Girifalco and OPLS-AA force fields were used for C_{60}. The carbon–carbon Lennard-Jones potential curves in the Girifalco and OPLS-AA force fields are shown in Fig. 3. Also shown in this figure is the total C_{60}–C_{60} potential energy assuming a uniform density of carbon atoms over the surface of a sphere the size of the C_{60} molecule. Due to the size difference between C60 molecules in the Girifalco and OPLS-AA force fields (7.10 Å versus 6.94 Å diameter, respectively), the well-depth of the total C_{60}–C_{60} interaction potential differs by a greater extent – almost 20% – than the carbon–carbon Lennard-Jones well depth.

Statistical averaging of fluctuating thermodynamic variables was carried out only when these variables ceased to display systematic variations with time, which typically took less than 1 ns for the P3HT-monomer simulations and less than 2 ns for the P3HT-decamer simulations. All reported statistical errors are two standard errors in the mean. [26]

Results and Discussion

Details of all of the simulations carried out are given in Table 1. Some simulations were also carried out for larger systems of longer P3HT chains of length 14 for the same blend ratios (using 100 P3HT 14-mers and 256 C_{60} molecules), which yielded essentially the same thermodynamic data as the decamer simulations, indicating that the results of the decamer simulations are representative of simulations of longer polymer chains.

As illustrated qualitatively in Figure 2c, which is typical of the configurations of all of the blend systems at all temperatures simulated for the simulations using the Girifalco model of C_{60}, no separation of P3HT and C_{60} phases was evident in any of these simulations. To quantify the degree of phase separation in the simulations, the normalised demixing or inhomogeneity parameter $\bar{\psi}_n$ was measured as a function of time. The demixing parameter can be defined in terms of the average local excess density of polymer in n^3 cells into which the cubic system has been divided by [27]

$$\bar{\psi}_n \equiv \frac{1}{n^3} \sum_{i=1}^{n^3} \left| \frac{\rho_i}{\langle \rho \rangle} - 1 \right| , \qquad (1)$$

where ρ_i is the local density of monomers in the i-th cell and ρ is the average system density of monomers. (The demixing can alternatively be measured in terms of the local fullerene density as well). $\bar{\psi}_n$ varies between 0 for a completely uniform phase and $2V_2/(V_1 + V_2)$ for two completely separated phases, where V_1 and V_2 are the volumes occupied by the

Table 1: Details of simulated systems containing P3HT monomers ($(3HT)_1$), P3HT decamers ($(3HT)_{10}$), and C_{60}.

System	T *	t_{tot} †	$\langle V \rangle_{Girifalco}$ ‡	$\langle V \rangle_{OPLS-AA}$ ‡
$(3HT)_1$	450	10	210.4	210.4
	500	10	225.7	225.7
	550	10	245.3	245.3
	600	10	270.3	270.3
$(3HT)_{10}$	450	10	171.8	171.8
	500	10	178.7	178.7
	550	10	186.6	186.6
	600	10	194.2	194.2
C_{60}	450	10	79.1	76.1
	500	10	79.3	76.7
	550	10	79.5	77.0
	600	10	79.6	77.2
$(3HT)_1$	450	40	279.0	275.6
+ C_{60}	500	40	291.5	288.9
	550	40	305.6	302.2
	600	40	322.0	318.3
$(3HT)_{10}$	450	40	245.6	240.3
+ C_{60}	500	40	252.0	246.8
	550	40	259.1	253.9
	600	40	267.2	261.5

* temperature (K); † total simulation time (ns); ‡ average system volume (nm^3)

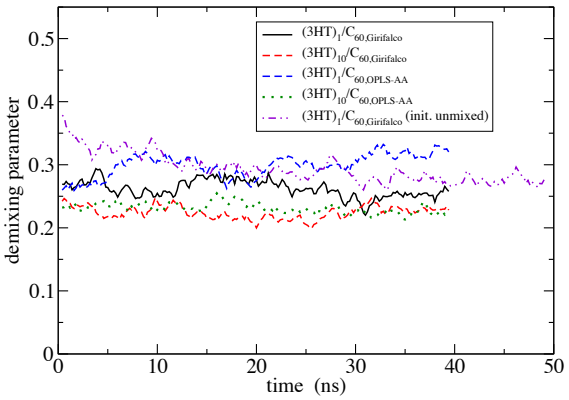

Figure 4: Demixing parameter $\bar{\psi}_n$ ($n = 4$) at 450 K for P3HT versus time starting from a homogeneously mixed system for P3HT-monomer/C_{60} (solid line) and P3HT-decamer/C_{60} (dashed line) using Girifalco C_{60} model and for P3HT-monomer/C_{60} (dot-dashed line) and P3HT-decamer/C_{60} (dotted line) using OPLS-AA C_{60} model and starting from phase-separated system for P3HT-monomer/C_{60} (dot-dot-dashed line) using Girifalco model. (Data has been averaged over 1-ns windows to reduce noise.)

two pure phases, although $\bar{\psi}_n$ cannot be zero for a system with fluctuating local densities; for a homogeneous system, it will be proportional to the standard deviation of the fluctuations in the local density, which decreases with the number of cells, n. The demixing parameter was measured as a function of time for the P3HT monomers in all of the P3HT/C_{60} blend simulations, which were started from initially homogeneously mixed systems. The cubic simulation box of length L was divided into n^3 cells of side length $l = L/n$, where n was 4, giving $l \approx 16$ Å, which is roughly 2.7 times the diameter of a P3HT monomer (similar results were obtained for $n = 3$ and 6). Figure 4 shows $\bar{\psi}_n$ as a function of time for the P3HT/C_{60} mixtures for the monomer and decamer systems using the two different force fields at 450 K, the lowest temperature simulated, at which phase separation would be expected to be most pronounced. Due to the small system size used, the data is noisy, but clear trends are evident. For simulations using the Girifalco C_{60} model, the demixing parameter in Figure 4 does not grow with time starting from an initially homogeneously mixed system, demonstrating that the mixtures do not phase separate within the time scale of the simulations (similar results were obtained at the other temperatures simulated). To verify that the absence of phase separation in the simulations was not simply due to kinetic frustration preventing the blend components from aggregating, simulations of the blend systems were carried at 450 K from 50 ns starting from a phase-separated configuration prepared by combining two pure systems of randomly placed molecules that was first cooled to 200 K. As shown in Figure 4, the demixing parameter for the P3HT-monomer/C_{60} system decreases monotonically with time, indicating that the P3HT/C_{60} blend has a tendency to mix with this force field, although longer simulations would be required to observe a completely homogeneously mixed equilibrium system.

On the other hand, the demixing parameter for the P3HT-monomer/C_{60} simulation using the OPLS-AA C_{60} model increases with time, indicating phase separation. The blend components in the P3HT-decamer/C_{60} systems did not exhibit significant enough mobility at 450 K to confirm or exclude phase separation of the blend components over the simulated time scale, with the demixing parameter approximately constant for both force fields. However, the results of the P3HT-monomer/C_{60} simulations, along with the statistical thermodynamic analysis based on the mixing enthalpy described below, suggest that the P3HT/C_{60} blend with the Girifalco C_{60} model is intrinsically miscible, whereas the blend with the OPLS-AA C_{60} model is intrinsically immiscible.

The respective miscibility and immisicibility of the P3HT-monomer/C_{60} blend using the Girifalco and OPLS-AA C_{60} models is illustrated in Figure 5, which shows the mixing of the initially phase-separated system for the Girifalco model and the demixing of the initially homogeneously mixed system for the OPLS-AA model.

To demonstrate further the absence of phase separation in the simulations using the Girifalco C_{60} model, the average of the enthalpy H was calculated as a function of temperature in the blend simulations from the averages of the internal energy U and system volume V using the definition of the enthalpy, $H = U + PV$,[28] where P is the pressure, which was constant in the simulations. The pressure–volume term was negligible compared with the energy term in the simulations carried out, and thus the enthalpy was roughly equal to the internal energy. A phase transition such as phase separation or crystallisation would manifest itself in a rapid change in the slope of the enthalpy as a function of temperature, which is clearly not evident in Figure 6, in which

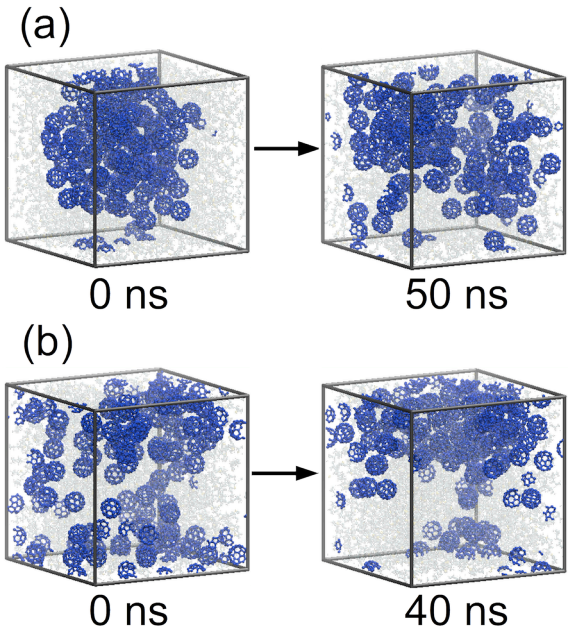

Figure 5: Configurations from start and end of simulations at 450 K and 1 atm starting from (a) a phase-separated configuration with Girifalco C_{60} model and (b) starting from a homogeneously mixed configuration with OPLS-AA C_{60}model. P3HT molecules are translucent for clarity.

the enthalpy of the mixture simulations varies linearly with temperature. The slope of the enthalpy versus temperature curve is the heat capacity at constant pressure, c_P,

$$c_P = \left(\frac{\partial H}{\partial T}\right)_{N,P} , \qquad (2)$$

which is 1.66 J/(g K) and 1.61 J/(g K), respectively, for the P3HT-monomer/C_{60} and P3HT-decamer/C_{60} mixtures in Figure 6. These values are consistent with those obtained alternatively from the fluctuations in the enthalpy [28] at each temperature according to

$$c_P = \frac{1}{k_B T^2}\left[\langle H^2\rangle_{NPT} - \langle H\rangle^2_{NPT}\right] , \qquad (3)$$

where $\langle\cdots\rangle_{NPT}$ denotes an average in the NPT ensemble. The heat capacities calculated using Equation (3) are shown in the inset of Figure 6. Also shown in the inset are the heat capacities of the pure P3HT-monomer, pure P3HT-decamer, and pure C_{60} systems, which are consistent with the experimentally measured heat capacities of P3HT (≈2.0 J/(g K)) [29] and C_{60} (1.11 J/(g K)) [30] at 450 K (below the heat capacity peak at the melting temperature of P3HT), providing further verification of the accuracy of the simulation model, although the OPLS-AA C_{60} model also gives a similar value for the C_{60} heat capacity. The heat capacities of the mixtures are approximately equal to the mass-weighted averages of the heat capacities of the pure components.

While the simulation results presented thus far for the Girifalco C_{60} model show that P3HT monomers or oligomers are quite miscible with C_{60} for the blend compositions typically used in P3HT/fullerene solar cells, whereas those for

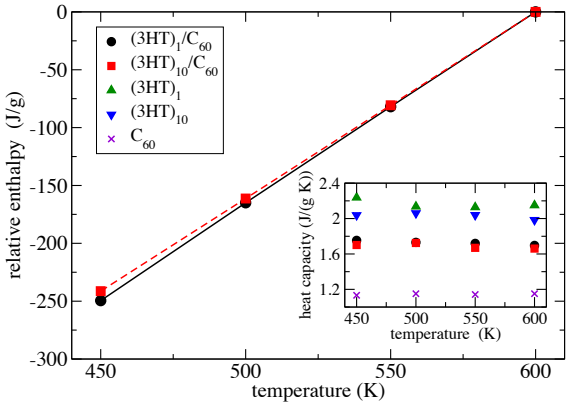

Figure 6: Enthalpy of P3HT-monomer/C_{60} mixture (circles) and P3HT-decamer/C_{60} mixture (squares) versus temperature (relative to value at 600 K) for simulations using the Girifalco C_{60} model. *Inset:* Specific heat capacity c_p at constant pressure of P3HT-monomer/C_{60} mixture (circles), P3HT-decamer/C_{60} mixture (squares), pure P3HT monomers (up triangles), pure P3HT decamers (down triangles), and C_{60} (crosses) versus temperature.

the OPLS-AA C_{60} model indicate that such blends are immisicible, these conclusions cannot be directly extrapolated to mixtures of C_{60} with P3HT polymers, for which diminished miscibility can be expected due to the decrease in the entropy of mixing of polymers with chain length. [13] Although atomistic simulations of polymeric blends are computationally prohibitive, the simulation results for monomeric and oligomeric systems can be combined with statistical thermodynamical arguments to predict the miscibility of amorphous mixtures of polymeric P3HT and C_{60}.

The Gibbs free energy of mixing, ΔG_{mix}, of two pure components to form a single homogeneous phase can be related to the enthalpy of mixing, ΔH_{mix}, entropy of mixing, ΔS_{mix}, and temperature, T, by

$$\Delta G_{mix} = \Delta H_{mix} - T\Delta S_{mix} . \qquad (4)$$

Assuming that the main contribution to the entropy of mixing is the change in configurational entropy, which can be computed from Flory–Huggins theory, [13] theory, ΔS_{mix} will be strictly positive for all polymer chain lengths. The enthalpy of mixing, ΔH_{mix}, can be estimated from the monomer and oligomer simulations that were carried out (for the homogeneously mixed systems), as the enthalpy should be dominated by the change in pairwise interactions between P3HT monomers and C_{60} upon mixing, which should be approximately independent of the polymer chain length. The enthalpy of mixing was obtained from the simulations using

$$\Delta H_{mix} = \Delta U_{mix} + P\Delta V_{mix} , \qquad (5)$$

where

$$\Delta f_{mix} = \langle f\rangle_{P3HT/C_{60}} - [\langle f\rangle_{P3HT} + \langle f\rangle_{C_{60}}] , \qquad (6)$$

$f = H, U,$ or V, and $\langle\cdots\rangle_{P3HT/C_{60}}$, $\langle\cdots\rangle_{P3HT}$, and $\langle\cdots\rangle_{C_{60}}$ denote ensemble averages over the homogeneously mixed blend system and corresponding pure P3HT and pure C_{60}

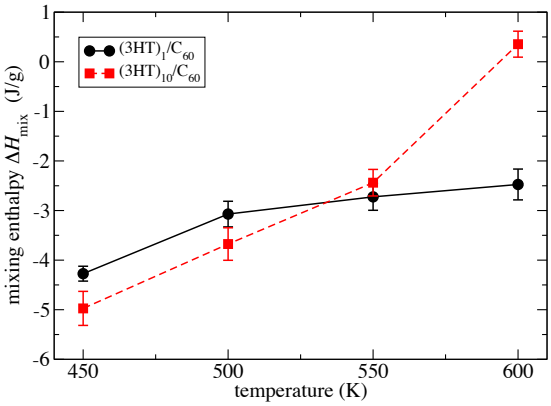

Figure 7: Enthalpy of mixing of P3HT-monomer/C_{60} (circles) and P3HT-decamer/C_{60} (squares) systems versus temperature for simulations using the Girifalco C_{60} model.

systems, respectively. As in the enthalpy calculations in Figure 6, the pressure–volume term in Equation (5) was small in all of the simulations carried out compared with the energy term. The calculation in Equation 6 involves the subtraction of two large numbers to yield a much smaller number and in general involves large errors; due to the large fluctuations in the bonded energies, the energy U in Equation 6 was approximated as the non-bonded pair energy in the simulations to reduce these errors. In any case, the non-bonded energy is expected to make a much more significant contribution than the bonded energy to the thermodynamics of mixing of amorphous blends.

The mixing enthalpy calculated from the simulations using the Girifalco C_{60} model is shown in Figure 7. The calculated mixing enthalpies for the P3HT-monomer/C_{60} and P3HT-decamer/C_{60} simulations overlap at all temperatures except 600 K, suggesting that, for the blend composition simulated, the mixing enthalpy is independent of chain length and thus that these results can be extrapolated to polymeric systems. (Note that the similiar mixing enthalpies for the monomer and decamer systems does not imply that the polymer/fullerene interactions are the same in these systems, which they are not, but simply that the change in the interactions upon mixing are similar.) Furthermore, within the error bars, ΔH_{mix} for both systems at all temperatures is negative and thus from Equation 4, the Gibbs free energy of mixing, ΔG_{mix}, will be negative at all of the temperatures simulated. This analysis for the simulations using the Girifalco C_{60} model does not account for the effects of crystallisation of either of the blend components, but does suggest that the amorphous P3HT/C_{60} mixtures should be miscible for the blend compositions and temperatures typically used in processing organic photovoltaics.

The origin of the negative mixing enthalpy in the simulations appears to be the overall closer packing in the mixture compared with the pure component systems, which results in an approximately 2.5% decrease in the total average volume in the case of P3HT-decamer/C_{60} blend upon mixing for all the temperatures studied. The closer proximity of the molecules appears to lead to stronger cohesive interactions: carrying out simulations of the same blend system with its volume constrained to be equal to the total volume of the pure P3HT and pure C_{60} systems results in mixing energies that are of similar order of magnitude but positive, instead of negative, in sign. The higher density in the blend is likely due to the ability of the smaller P3HT monomer to occupy the interstitial spaces between the larger C_{60} molecules that are present in the pure C_{60} phase, which leads to a smaller free volume in the blend. The closer packing of P3HT monomer units with C_{60} molecules than C_{60} molecules with each other can be clearly seen in the intermolecular radial distribution functions, which are plotted for a similar atomistic force field in Ref. 14.

The strength of the intermolecular non-bonded interactions also play a role in determining the miscibility of the blend, as indicated by the contrasting behaviour of the simulations using the OPLS-AA C_{60} model. Since the positive entropy of mixing is expected to decrease in magnitude with polymer chain length,[13] the Gibbs free energy of mixing for the systems using the OPLS-AA C_{60} model should become more positive with increasing polymer chain length. Since the demixing of the P3HT-monomer/C_{60} system suggest that the free energy of mixing is already positive for monomers, this thermodynamic analysis indicates that amorphous P3HT polymers should not mix with C_{60}.

Experimental thermodynamic data on the mixing of P3HT and C_{60} is not widely available. Although the simulation results for P3HT/C_{60} mixtures cannot be directly compared with experimental data for the more extensively studied P3HT/PCBM blend,[8–10,12] the substantial miscibility of amorphous P3HT and C_{60} predicted by the simulations using the Girifalco C_{60} model is qualitatively consistent with that observed experimentally for P3HT/PCBM mixtures. Future work involving atomistic simulations of P3HT/PCBM mixtures is planned to verify these conclusions. However, the contrasting predictions based on the simulations using the OPLS-AA C_{60} model, which differs only slightly from the Girifalco model, indicates that the homogeneously mixed and separated P3HT/C_{60} phases are close to coexistence under the conditions simulated. These contradictory results also indicate a need for greater scrutiny and benchmarking against experimental simulation data of atomistic simulation force fields of P3HT/fullerene blends, as well as the coarse-grained simulation force fields that are based on these atomistic force fields.

Conclusions

Using molecular dynamics simulations and statistical thermodynamics, it has been shown that amorphous P3HT/C_{60} blends are either miscible or immisicible for typical blend compositions and processing conditions used in organic photovoltaics, depending on which of two slight different force fields are used. The former finding is consistent with recent experimental measurements on the thermodynamics and microstructure of P3HT/fullerene blends and suggests that the phase separation of blends of regioregular P3HT and fullerenes is driven by polymer crystallisation. The inconsistency between the results for the different two force fields indicates that these blends are close to phase coexistence between the separated and homogeneously mixed phases and suggests that care must be taken in interpreting simulation data on P3HT/fullerene blends.

Acknowledgments

This work was supported by an award under the Merit Allocation Scheme on the NCI National Facility at the ANU and used computational resources at eResearch SA.

References

[1] C. J. Brabec, S. Gowrisanker, J. J. M. Halls, D. Laird, S. Jia, S. P. Williams, *Adv. Mater.* **2010**, *22*, 3839.

[2] C. J. Brabec, M. Heeney, I. McCulloch, J. Nelson, *Chem. Soc. Rev.* **2011**, *40*, 1185.

[3] C. Müller, T. A. M. Ferenczi, M. Campoy-Quiles, J. M. Frost, D. D. C. Bradley, P. Smith, N. Stingelin-Stutzmann, J. Nelson, *Adv. Mater.* **2008**, *20*, 3510.

[4] N. D. Treat, M. A. Brady, G. Smith, M. F. Toney, E. J. Kramer, C. J. Hawker, M. L. Chabinyc, *Adv. Energy Mater.* **2011**, *1*, 82.

[5] N. D. Treat, A. Varotto, C. J. Takacs, N. Batara, M. Al-Hashimi, M. J. Heeney, A. J. Heeger, F. Wudl, C. J. Hawker, M. L. Chabinyc, *J. Am. Chem. Soc.* **2012**, *134*, 15869.

[6] F. C. Jamieson, E. B. Domingo, T. McCarthy-Ward, M. Heeney, N. Stingelin, J. R. Durrant, *Chem. Sci.* **2012**, *3*, 485.

[7] P. Westacott, J. R. Tumbleston, S. Shoaee, S. Fearn, J. H. Bannock, J. B. Gilchrist, S. Heutz, J. deMello, M. Heeney, H. Ade, J. Durrant, D. S. McPhail, N. Stingelin, *Energy Environ. Sci.* **2013**, *6*, 2756.

[8] D. Chen, A. Nakahara, D. Wei, D. Nordlund, T. P. Russell, *Nano Lett.* **2011**, *11*, 561.

[9] D. R. Kozub, K. Vakhshouri, L. M. Orme, C. Wang, A. Hexemer, E. D. Gomez, *Macromolecules* **2011**, *44*, 5722.

[10] J. Y. Kim, C. D. Frisbie, *J. Phys. Chem. C* **2008**, *112*, 17726.

[11] B. Watts, W. J. Belcher, L. Thomsen, H. Ade, P. C. Dastoor, *Macromolecules* **2009**, *42*, 8392.

[12] B. A. Collins, E. Gann, L. Guignard, X. He, C. R. McNeill, H. Ade, *J. Phys. Chem. Lett.* **2010**, *1*, 3160.

[13] M. Rubinstein, R. H. Colby, *Polymer Physics* **2003** (Oxford University Press: Oxford).

[14] D. M. Huang, R. Faller, K. Do, A. J. Moulé, *J. Chem. Theory Comput.* **2010**, *6*, 526.

[15] C.-K. Lee, C.-W. Pao, C.-W. Chu, *Energy Environ. Sci.* **2011**, *4*, 4124.

[16] D. M. Huang, A. J. Moulé, R. Faller, *Fluid Phase Equilibria* **2011**, *302*, 21.

[17] S. J. Plimpton, *J. Comput. Phys.* **1995**, *117*, 1, `LAMMPS` Molecular Dynamics Simulator: http://lammps.sandia.gov.

[18] L. A. Girifalco, *J. Phys. Chem.* **1992**, *96*, 858.

[19] K. N. Schwarz, T. W. Kee, D. M. Huang, *Nanoscale* **2013**, *5*, 2017.

[20] V. Marcon, G. Raos, *J. Am. Chem. Soc.* **2006**, *128*, 1408.

[21] W. L. Jorgensen, D. S. Maxwell, J. Tirado-Rives, *J. Am. Chem. Soc.* **1996**, *118*, 11225.

[22] D. J. Price, J. D. Roberts, W. L. Jorgensen, *J. Am. Chem. Soc.* **1998**, *120*, 9672.

[23] W. L. Jorgensen, N. A. McDonald, *THEOCHEM* **1998**, *424*, 145.

[24] S. B. Darling, M. Sternberg, *J. Phys. Chem. B* **2009**, *113*, 6215.

[25] K. Hedberg, L. Hedberg, D. S. Bethune, C. A. Brown, H. C. Dorn, R. D. Johnson, M. De Vries, *Science* **1991**, *254*, 410.

[26] M. P. Allen, D. J. Tildesley, *Computer Simulation of Liquids* **1987** (Clarendon: Oxford).

[27] P. I. Hurtado, P. Chaudhuri, L. Berthier, W. Kob, *AIP Conf. Proc.* **2009**, *1091*, 166.

[28] L. E. Reichl, *A Modern Course in Statistical Physics* 2nd edn., **1998** (Wiley-Interscience: New York).

[29] S. Hugger, R. Thomann, T. Heinzel, T. Thurn-Albrecht, *Colloid Polym. Sci.* **2004**, *282*, 932.

[30] Y. Jin, J. Cheng, M. Varma-Nair, G. Liang, Y. Fu, B. Wunderlich, X. D. Xiang, R. Mostovoy, A. K. Zettl, *J. Phys. Chem.* **1992**, *96*, 5151.